Landscape evolution of the Bolivian Amazon controlled by uplift events dated 13,000, 10,000 and 6000 cal yr BP

Quaternary Science Reviews 352 (2025) 109197

Contents lists available at ScienceDirect

Quaternary Science Reviews

journal homepage: www.elsevier.com/locate/quascirev

Landscape evolution of the Bolivian Amazon controlled by uplift events dated 13,000, 10,000 and 6000 cal yr BP

U. Lombardo [a,b,*], L. Becerra-Valdivia [c], G.A. Butiseacă [a], C. Bronk Ramsey [d], J. Ibañez-Insa [e], H. Veit [f], F. Mayle [g]

[a] Institute of Environmental Science and Technology, Autonomous University of Barcelona, Barcelona, Spain
[b] Department of Prehistory, Autonomous University of Barcelona, Barcelona, Spain
[c] Department of Anthropology and Archaeology, University of Bristol, Bristol, UK
[d] School of Archaeology, University of Oxford, Oxford, UK
[e] Geosciences Barcelona (GEO3BCN), CSIC, Barcelona, Spain
[f] Department of Geography, University of Bern, Bern, Switzerland
[g] Department of Geography and Environmental Science, University of Reading, Berkshire, Reading, UK

ARTICLE INFO

Handling editor: P Rioual

ABSTRACT

The Llanos de Moxos in the Bolivian Amazon, the second largest South American wetland, hosts many endemic species and a rich archaeological record that spans the entire Holocene. Despite its ecological and archaeological importance, very little is known about its Holocene environmental history. A growing body of evidence suggests that neotectonics played an important role in shaping its modern landscape and controlling past flooding dynamics, but the chronology and vertical displacements of past tectonic events are still largely unknown. Here, we present new data from a core taken at Lake Oceano, a large ria lake in the northern part of the Llanos de Moxos. To identify changes in the lithology and environment, we performed a battery of analyses, such as XRF scanning, mineralogy, granulometry, C/N and C and N stable isotopes, and also built an age-depth model using eighteen radiocarbon dates obtained from accelerator mass spectrometry (AMS) determinations. Based on the sedimentology and chemical analyses, we identified three major disturbances in the lake sedimentation that we interpret as positive tectonic events (i.e., tectonic uplifts). The first identified event occurred at approximately 13,400 cal yr BP and led to the formation of the lake by blocking the river course. A second uplift event took place around 10,000 cal yr BP, accompanied by a significant change in the geochemistry of the lake sediments. Furthermore, we have verified a third event at 6000 cal yr BP, previously recognized as responsible for the onset of Lake Rogaguado (aprox. 100 km NE of Lake Oceano), one of the largest lakes in South America. Overall, we show that ria lakes can provide key sedimentary archives to reconstruct the past timing and intensity of tectonic events. We discuss the interplay between tectonics and climate, highlighting the connection between tectonics and the region's flood history, with crucial implications for the interpretation of both archaeological and palaeoecological records throughout the Holocene.

1. Introduction and study area

The Llanos de Moxos (LM) is located in the Bolivian Amazon and comprises an extended seasonally flooded savannah that covers most of the southern Andean foreland basin. The LM is the second largest South American wetland after the Pantanal (Junk, 2013). It hosts many endemic species and a rich archaeological record that spans the entire Holocene (Langstroth, 2011; Lombardo et al., 2011, 2013b). This is one of the earliest world centres of plant domestication (Lombardo et al., 2020). The ecology and archaeology of this area have been shaped by how plants, animals, and humans have adapted to its edaphic and hydrological conditions (Langstroth, 2011; Lombardo et al., 2013a; Mayle et al., 2007; Navarro, 2011). While these conditions have evolved over the Holocene, much remains unknown about the timing, direction, and extent of the changes (Dumont and Fournier, 1994; Hanagarth, 1993; Lombardo, 2014, 2016; Lombardo and Grützner, 2021). The landscape and ecology of the LM are mostly controlled by the seasonal flood cycle (Junk et al., 1989). This depends on two independent factors: climate

* Corresponding author. Building ICTA-ICP, Carrer de les columns Universitat Autònoma de Barcelona Bellaterra, 08193, Barcelona, Spain.
E-mail address: Umberto.Lombardo@uab.cat (U. Lombardo).

https://doi.org/10.1016/j.quascirev.2025.109197
Received 4 July 2024; Received in revised form 10 January 2025; Accepted 11 January 2025
Available online 31 January 2025

and topography. Intensity and seasonality of precipitation control the water input (Ronchail et al., 2005), while the topography and sediment/bedrock permeability control the drainage of the basin (Lombardo, 2014; Ronchail et al., 2005). The combination of precipitation, runoff and water table depth is therefore responsible for the extent and duration of the seasonal flood and, in turn, for the sedimentation rates, flood pulse, land cover, nutrient turnover, biodiversity, and human adaptation.

1.1. Geological background

The LM is bordered by the Andes to the southwest, the Brazilian Shield to the northeast, and the southern edge of the Fitzcarrald Arch to the north (Fig. 1). The Amazonian foreland is composed of two subsiding basins, one to the north and one to the south (i.e., the Northern and Southern Amazonian Foreland Basins). The two are separated by the Fitzcarrald Arch, a broad uplifted tectonic block resulting from the flat slab subduction of the oceanic Nazca Ridge (Espurt et al., 2007, 2010; Roddaz et al., 2005). The Andean orogenic load, resulting from the collision between the Nazca and South American plates, created a forebulge structure that migrated eastwards (Horton et al., 2022; Rocha et al., 2022). The migration of the forebulge created parallel faults with the Andes. The LM covers most of the foredeep of the southern Andean Amazonian foreland basin and is close to the margin of the Andean forebulge. The dynamics of the LM are driven by the interplay between the uplift of the Fitzcarrald Arch, the subsidence of the main basin and the migration of the forebulge, which induced two deformation directions: one parallel with the Andes and one parallel with the Fitzcarrald Arch. Recent analyses of the topography of the LM have shown that this tectonic setting is expressed on the surface by the presence of several normal and blind faults (Lombardo and Grützner, 2021).

1.2. Hydrology and climatic parameters

The central and southern LM are characterised by large and seasonally-flooded savannahs criss-crossed by meandering rivers and palaeo rivers. The climate is characterised by two periods with opposite hydrological budgets: a rainy season (from October to April) and a dry season (May to September). During the rainy season, precipitation can reach 500 mm/month and decrease drastically during the dry season down to <50 mm monthly precipitation (Hanagarth, 1993). The average slope of the central LM is approximately 10 cm per km, resulting in a very slow movement of the surface water during the rainy season. The savannah's floor is dominated by clayey soils, very poor in nutrients and impermeable (Boixadera et al., 2003; Lombardo et al., 2015; Rodrigues et al., 2017). This, combined with the precipitation seasonality, make them unsuitable for trees, which cannot withstand the contrast between months of anoxic conditions during which the savannah is flooded (i.e., December to May) and months of extremely dry conditions (i.e., July to October) (Mayle et al., 2007). Hence, the forested areas are relegated to the higher parts of the landscape, mostly fluvial levees and palaeo levees, that don't get flooded or are flooded for only short periods of time. To the north, the floodplain transitions into the relatively well drained Cerrado Beniano, dominated by lateritic soils and crusts. In contrast to the floodplains in the south, this area is characterised by a gentle topography with hills of about 20–30 m in elevation. Here, the forest grows in the lower parts of the landscape, mostly in the small valleys between the lateritic hills, where sediment accumulation provides enough humidity and room for tree roots to grow (Lombardo, 2014). These small valleys are the result of stream incision. It is important to note that the distal/lower part of these valleys is nowadays infilled with sediments and in some instances, like the very case of Lake Oceano, host a lake. The Cerrado Beniano is well above the level of the seasonal floods. Hence, here, the forest-savannah ecotone is determined

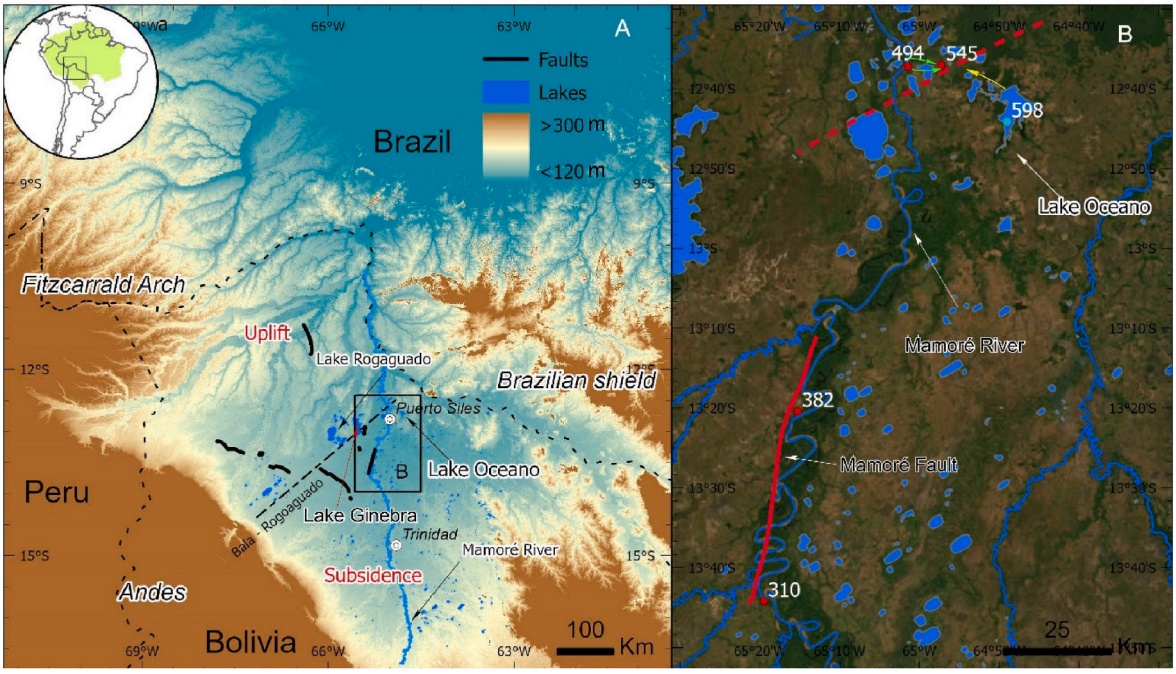

Fig. 1. In panel A, the geologic and topographic setting of the Bolivian Amazon. The northern part, which is the southern rim of the Fitzcarrald Arch is uplifting, while the southern part, the Andean forebulge, which mostly overlaps with the Llanos de Moxos (blueish area in panel A), is sinking. The large lakes of tectonic origin are aligned along the boundary between the two opposing geodynamic settings, which roughly run along the Bala-Rogaguado line, a structural axis identified in Dumont and Fournier (1994). The black box shows the location of part B. Panel B shows the locations of the cores (red dots) used in the present study, together with the active faults (red lines). The green and yellow arrows mark the directions of sediment and water movement in the area, respectively. The digital elevation model in panel A is based on NASA Shuttle Radar Topography Mission (SRTM) (2013). Shuttle Radar Topography Mission (SRTM) Global. Distributed by OpenTopography. https://doi.org/10.5069/G9445JDF. Satellite imagery in panel B is provided by ESRI under the ArcGIS Pro licence. (For interpretation of the references to colour in this figure legend, the reader is referred to the Web version of this article.)

primarily by soil properties and local precipitation and is relatively independent from the LM's flood regime. Some of the largest lakes in the LM, including Lake Rogaguado and Lake Oceano, are located here (Fig. 1). This area coincides with the southern rim of the uplifting Fitzcarrald Arch.

1.3. Landscape evolution and depositional system

Despite new evidence suggesting that neotectonics is an ongoing driver of landscape evolution in the Bolivian Amazon (Lombardo, 2014; Lombardo and Grützner, 2021), the timing, uplift rate and impact of neo-tectonic movements are still largely unknown. The geodynamic setting of the LM is directly controlled by two opposing ongoing processes (Fig. 1). To the southwest, closer to the Andes, subsidence and normal faulting—due to the load of the Andes that flexes the crust and sediment compaction accommodate the deposition of new fluvial sediments; while, to the north, the southern rim of the Fitzcarrald Arch's uplift (Espurt et al., 2007; Regard et al., 2009; Roddaz et al., 2005) causes denudation, fluvial incision and impeded drainage (Lombardo, 2014, 2016; Lombardo and Grützner, 2021). Several geomorphological expressions of the ongoing uplift of the northern part of the LM have already been described, mapped and in a very few instances dated (Dumont, 1993a, 1993b, 1996; Dumont and Fournier, 1994; Espurt et al., 2010; Lombardo, 2014). Downstream uplifts have a major effect on both active and palaeo rivers (Nichols and Fisher, 2007; Schumm et al., 2002). In the case of palaeochannels, the downstream uplift can invert the slope of the channel and cause the formation of lakes along a portion of the fluvial valley (Lombardo, 2014; Lombardo and Grützner, 2021). In some instances, the increased overbank sedimentation caused by the elevation of a river base-level can dam a lateral valley and create a lake. These lakes are called *rias* (Dumont, 1993a; Dumont and Guyot, 1993) and they are usually driven by positive tectonic movements.

The inverted palaeochannels and ria lakes of Amazonian Bolivia offer unique opportunities to reconstruct the timing and uplift rates of neotectonic processes that affected the LM Basin. The formation of large lakes such as lake Rogaguado and lake Ginebra has been caused by the inversion of the slope of abandoned palaeochannels resulting from the tilting of the tectonic block towards the north (Lombardo, 2014), likely associated with blind faults. Blind faults are common in areas undergoing compressional stress, which have rocks that deform ductile overlying rocks that deform brittle, in our case consolidated rocks in the basement of the basin, covered by unconsolidated Quaternary sediments. These faults do not break through the surface and are related to bigger strike-slip faulting processes. In the case of the LM, the compression takes place in the front of Fitzcarrald Arch, that is pushed in turn by the indentation of the Nazca plate. A strike slip component was already identified by Lombardo and Grützner (2021). The southern shorelines of Lakes Rogaguado and Ginebra coincide with a sharp change in the slope of the palaeo valley where the lake formed and are aligned with the portion of the River Yata located between two 90° turns, suggesting the presence of a fault (Fig. 10 in Lombardo, 2014). Active rivers are also heavily impacted by the downriver uplift. The longitudinal topographic profile of the Mamoré River, its gallery forest and meandering pattern, reveal the presence of two knickpoints, one located at the town Puerto Siles, which occurs at the boundary between the seasonally-flooded plains of the south and the hilly lateritic landscape of the Cerrado Beniano to the north, and the other in Guayaramerín (Fig. 5 in Lombardo, 2014). In its northern reach, right after the connection with the Iténez (or Guaporé) River, the Mamoré River flows along the contact of the southern rim of the Fitzcarrald Arch with the Brazilian shield.

1.4. Aims and rationale

It has been hypothesised that the uplift/tilting that formed the Puerto Siles and Guayanamerín knickpoints caused backward sedimentation, which, by damming lateral valleys, formed the lakes Agua Clara, Largo, Oceano and the other small ria lakes at the eastern margin of the Mamoré River (Lombardo, 2014). To test this hypothesis, we cored Mamoré River's overbank deposits and compared granulometric and mineralogical characteristics of two cores taken along the river to the south of Lake Oceano, and two cores taken from the land strip that separates Lake Oceano from the Mamoré River. We assumed that, 1) if Lake Oceano was formed by the damming of a valley by sediments deposited by the Mamoré River, the four cores should show similar characteristics; and 2) If the deposition along the Mamoré banks was driven by increased river discharge caused by increased precipitation, deposited sediments should be consistent with a relatively high-energy depositional environment. Lake Oceano was also cored, to check if uplift events could cause changes in the catchment of the lake and further influence the geochemistry of the lake sediments. We discuss the new data in the light of already published information from inverted palaeochannels (Lombardo, 2014; Lombardo and Grützner, 2021), and provide the first assessment of uplift rates in the northern LM, together with a reconstruction of the main neo-tectonic events that characterise the landscape evolution of the Llanos de Moxos since the late Pleistocene.

2. Methodology

2.1. Sampling

Lake sediments were collected using a Livingston piston corer in August 2019. To obtain a continuous record, two cores were taken, ca. 10 m apart from each other, with a 50 cm overlap. Aluminium core tubes were sealed after recovery and opened in the laboratory using an angle grinder. Cores were split into two halves, one used for X-ray scanning and storage, while the other half for sediment sampling for geochemical analyses. After opening, cores were stored in the fridge between 2 - 4 °C.

2.2. Chronology

The age-depth model (Supplementary Fig. 1) of the sediment core was calculated based on sixteen bulk-sediment samples, dated as base-insoluble fractions (Oxford Radiocarbon Accelerator Unit (ORAU) pretreatment code (Pcode) SRa; 'humin'), with two samples (nos. 13 and 14) receiving additional base-soluble measurements (ORAU Pcode SRb; 'humic acids') for comparison. Bulk samples were used for dating due to insufficient terrestrial plant macrofossils or macroscopic charcoal. The absence of carbonate bedrock means that the hard-water effect is likely to be negligible. Dates were entered into a Poisson deposition model within OxCal software (4.4), with a k parameter (k_0) of 100, an interpolation rate of 200 (where an output is given every 5 mm), and a log_10 (k/k_0) of U(-2,2). The latter allows k to vary by two orders of magnitude in either direction (from 0.01 to 100). In addition, a 'General' outlier model was applied to all dates, with each being given a 5% prior probability of being an outlier (Bronk Ramsey, 2009). Calibration was undertaken using IntCal and SHCal calibration curves (Hogg et al., 2020; Reimer et al., 2020). A complete list of the dated samples and the code used are provided in the Supplementary Information (Table 1).

2.3. Grain size analysis

Samples were treated with H_2O_2 and HCl respectively, to remove organic matter and carbonates. Additionally, iron oxides were removed using the oxalate, citrate, bicarbonate (DCB) method (Pansu and Gautheyrou, 2006) from all the Rio Mamoré overbank deposits (cores 545, 494, 382 and 310). Grain size was measured using a laser diffraction particle size analyser Horiba LA950 at Ciencies del Mar, CSIC.

2.4. Elemental analysis

Elemental analysis was performed immediately after splitting the

lake cores by x-ray fluorescence (XRF) scanning at the University of Bern using an ITRAX-XRF core scanner (Cox Ltd., Sweden) set to 10 kV, 10 mA and 20 s of exposure time at 5 mm increments.

2.5. Mineralogical analysis

Whole-rock powder x-ray diffraction (XRD) measurements were performed at the XRD Laboratory of Geosciences Barcelona (GEO3BCN-CSIC). For this purpose, samples were pulverised and homogenised manually. The XRD scans were acquired by using a Bruker D8-A25 diffractometer equipped with a Cu X-ray source (Cu Kα radiation) and a LynxEye position sensitive detector (PSD). The scans were recorded between 4° and 60° in 2θ with a 0.035° step size and equivalent counting times of 384 s. Phase identification was carried out by using the DIFFRAC.EVA software from Bruker together with the Powder Diffraction File (PDF-2) database, which is released and maintained by the

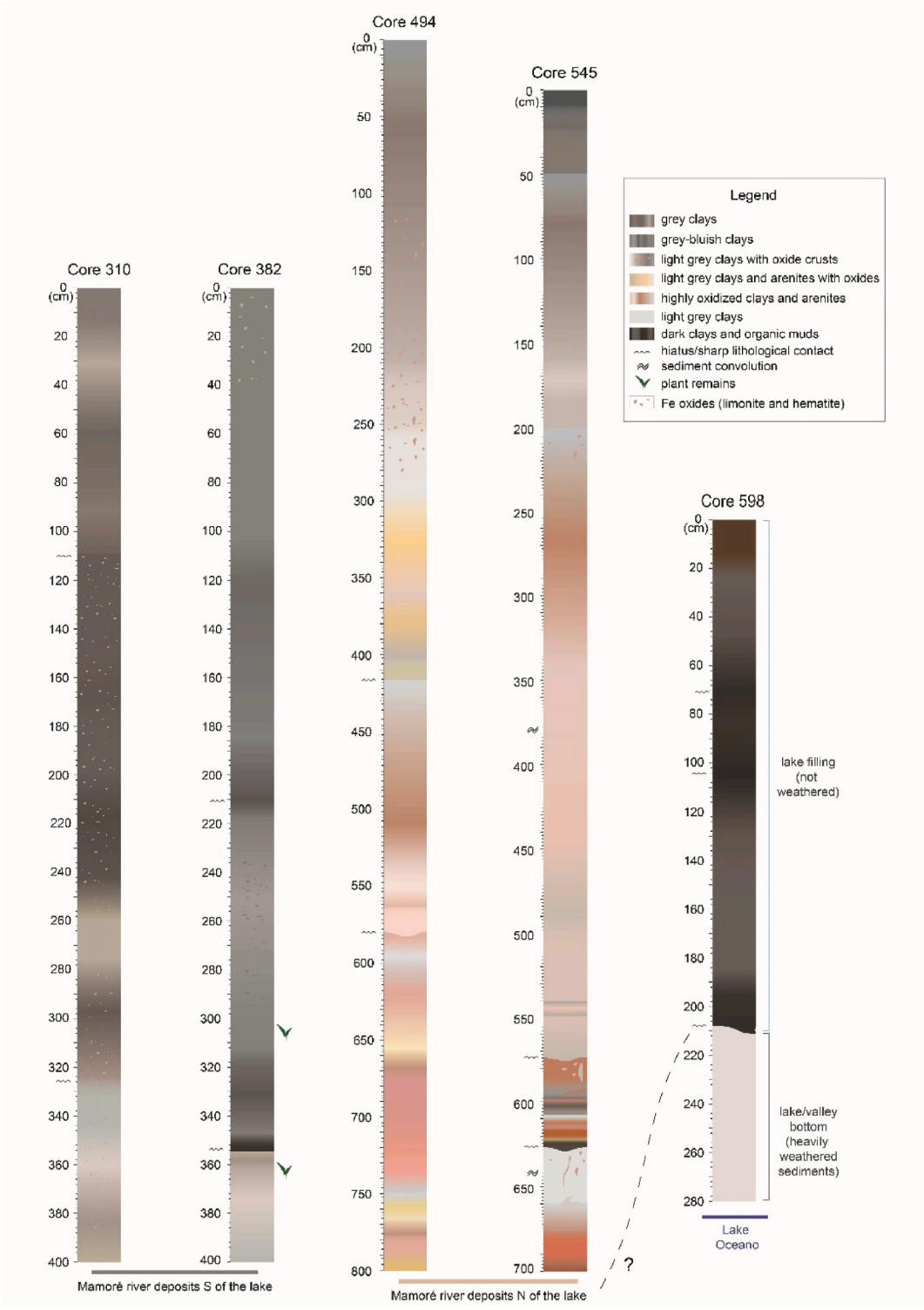

Fig. 2. Lithological columns for cores 310, 382, 494, 545, and 598, and core correlation. The lithologies indicate different sources for the sediments in and around the lake.

International Centre for Diffraction Data (ICDD, https://www.icdd.com/). To obtain quantitative information about the whole-rock mineralogy of the investigated samples, semi-quantitative phase analyses based on the reference intensity ratio (RIR) method were carried out. For this purpose, RIR values given in the PDF-2 database were used.

2.6. Stable isotopes

Carbon and nitrogen stable-isotope ratios ($\delta^{13}C$ and $\delta^{15}N$) were determined with a Flash IRMS elemental analyser, coupled to a Delta V Advantage IRMS via a Conflow IV interface. IAEA600 and a laboratory reference material calibrated with IAEA600 were used as standards. The isotopic ratios were reported relative to the Vienna Peedee Belemnite (VPDB) standard.

3. Results and interpretation

3.1. Core description and granulometry

A total of five cores (Fig. 2) were collected to track changes in the sedimentology and depositional system of the study area. A 2.8 m long core (Supplementary Fig. 3) was retrieved from Lake Oceano (location 598; Fig. 1B). The water column at the time of coring was 3.1 m. Mamoré River's overbank deposits were cored on the land strip separating Lake Oceano from the Mamoré River. Four soil cores were taken in this area, two between the lake and the Mamoré River (locations 545 and 494), and two others south of the lake (locations 382 and 310; Fig. 1).

Core 598. The bottom part of lake core 598 comprises white, clayey material. On top of this white sediment, after a sharp contact, the lacustrine sedimentation begins with a quite homogeneous, ~1 m thick layer of dark organic clay (2.08–1.0 m depth). Two sharp transitions towards darker colour are clearly visible at 1.0 m and at 75 cm depth. Another sharp transition, this time towards grey clays, is visible at 50 cm depth. Further up the core, sediments become gradually darker until 20 cm depth, where the material becomes loose and reddish (Fig. 2).

Core 545 measures 7 m and comprises very reddish material, mostly sand/coarse silt, in the first half metre, overlain by 50 cm of whitish sand/coarse silt. The rest of the core comprises fine, whitish and greyish material with iron oxides (hematite and limonite). The uppermost 1.5 m comprises organic clay (Fig. 2), probably deposited as infilling of the lake shore.

Core 494 is the longest core, with a recovery of ~8 m. It starts with heavily oxidised layers of sand/arenite and clay from 8.0 to 5.7 m depth, followed by 2 m of grey clay with red oxides and 1 m of grey clay/silt with orange oxides. These iron oxides probably result from the oscillation of the water table linked to the water level of the river, with periods of aerial exposure and oxidation. From 2.9 m depth, cracks filled with organic material appear, confirming the exposure to seasonal dry periods. The uppermost metre contains organic rich clay/silt with yellow/orange oxides in the bottom half (Fig. 2).

Core 382 is 4 m long. Between 4 and 3.7 m depth the core is characterised by greyish bluish silty sediments. After a sharp boundary, there are silts with high amounts of plant remains and charcoal, followed by a thin, black layer between 3.6 and 3.55 m depth. From 3.55 to 3.2 m depth, sediments comprise dark clay/silt with limonite. Between 3.2 and 3 m depth there is a clay/silt layer very rich in organic matter, both charcoal and plant remains. The rest of the core, from 3 m depth to the surface, comprises dark clay/silt with varying amounts of organics and little to no evidence of oxidation (Fig. 2).

Core 310 is 4 m long. The lower part (approximately 400 to 250 cm) comprises grey and bluish clays, with limonitic oxidation. The middle part of the core comprises very organic clay/silt with red oxides (~240–110 cm). The upper part comprises brown clay/silt between 1 m and 50 cm depth, with a dark layer, likely a palaeosol, covered by laminated fluvial sand from 35 to 15 cm depth. The uppermost part comprises organic-rich fine silt (Fig. 2). Overall, the granulometry of core 310 is consistent with that of core 382 (Fig. 3), indicating similar water energy and sedimentation patterns, with fine material probably deposited during periods of low water discharge (i.e., end and beginning of the rainy season) and coarser material deposited during the higher discharge of the rainy season.

The location of core 545 shows the very same granulometry as that of core 494 for the first 3.5 m, including the trimodal distribution at 557 cm depth. However, in the upper 3.5 m, core 545 shows consistently finer sediments. Except for the basal samples from core 494 and 545, none of the samples show any significant amount of sand. This is not surprising given the fact that in the LM the suspended load is dominated by silts (Guyot et al., 1999).

Cores located along the river channel (310, 382 and 494), except for the sample at 557 cm depth in core 494, mostly comprise silt. The silt content decreases, while the clay fraction increases, moving away from the river channel (core 545) and sediments are mostly clay in the lake (core 598; Figs. 2, 3). The grain size distribution is mostly bimodal, with the coarser peak probably signalling deposition during particularly rainy years and higher discharge. Bi- and tri-modal distributions are more common in the soil cores than in the lake core, where a clearly bimodal distribution is visible only in the uppermost sample (Fig. 3).

3.2. Chronology

Eighteen dates from the lake core 598 were used to build the age-depth model of Lake Oceano (Supplementary Table 1; Supplementary Fig. 1). All the ages are stratigraphically consistent, except for one sample (Lab code OxA-X-3128-11), which is an outlier, probably due to contamination. Ages obtained for the different chemical fractions of the same sample (lab codes OxA-X-3128-19; OxA-X-3130-11) are slightly different ($\chi^2 = 4.7$; df = 1; p = 3.8), with the base-insoluble date being older. The difference is marginal, however, and the combined age for sample 13 is not identified as an outlier within the model. The basal age of the core 598, at a depth of 2.05 m, is in the range of 13,503–13,326 cal yr BP, which marks the lake onset. Sedimentation rates (Fig. 4) reach a maximum around 12,200 cal yr BP, followed by two sharp decreases at around 12,000 and 9000 cal yr BP. The first 80 cm of the lake sediments were deposited in approx. 1400 years; the following 55 cm were deposited in approx. 3000 years; and the uppermost 75 cm of sediments were deposited in 9000 years (Supplementary Fig. 2). The radiocarbon measurement from the plant remains of core 382 at a depth of 3.5 m provided an age between 13,085 and 12,905 cal yr BP for the burial of the plant remains, suggesting that the formation of Lake Oceano and the burial of the ancient gallery forest along the Mamoré River were synchronous.

3.3. Elemental and mineralogical analyses

Several commonly used elemental ratios, obtained by XRF, were calculated in order to show changes in the granulometry of the sediments (Si/Al; Zr/Rb), sources of detrital input (K/Ti), biogenic silica productivity (Si/Ti), and reducing conditions/oxygenation in the lake (Fe/Ti) (Davies et al., 2015) (Fig. 4). All elemental ratios mark important environmental changes (i.e., sharp increase in Si/Al and Zr/Rb ratios; sharp decrease in K/Ti, Si/Ti, and Fe/Ti ratios) at ca. 13,400 cal yr BP (the onset of lacustrine sedimentation), ca. 10,000 cal yr BP, and ca. 6000 cal yr BP, the latter coinciding with the formation of Lake Rogaguado caused by the uplift (Fig. 4; tectonic sketches) of the southern margin of the Fitzcarrald Arch (Dumont and Fournier, 1994; Giesche et al., 2021; Hanagarth, 1993; Lombardo, 2014). A peak in sedimentation rate at ca. 12,200 cal yr BP coincides with a small reduction in the K/Ti and Fe/Ti ratios, indicating a reduction in oxygenation and increased turbidity in the lake. A peak is visible in Fe/Ti and Si/Ti ratios around 13,000 cal yr BP, which coincides with a peak in Ar. Hence, it is likely an artefact due to a crack in the core surface (see Supplementary Fig. 4). Biogenic silica (Si/Ti) rises after 10,200 cal yr BP and remains

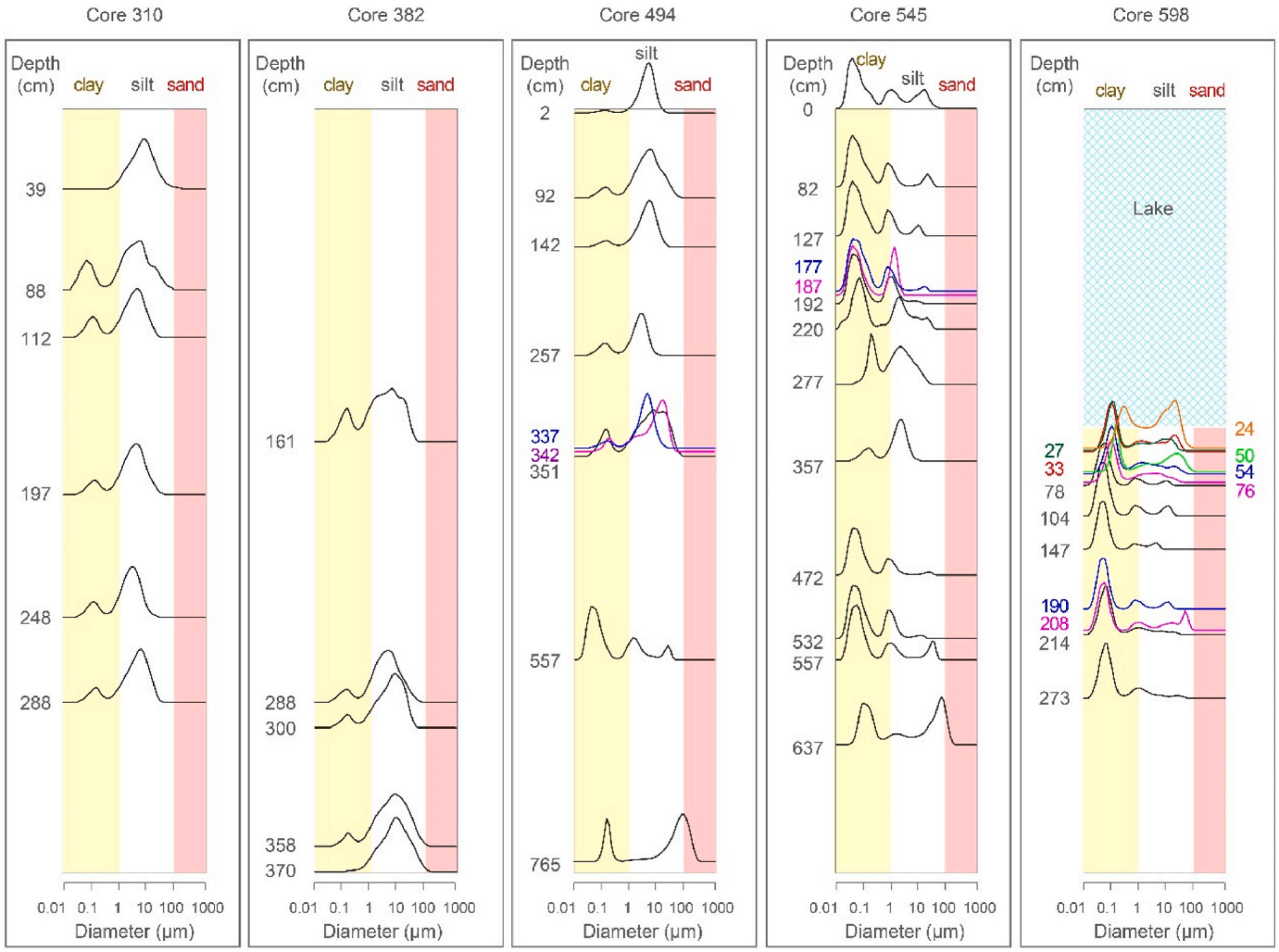

Fig. 3. Grain size distribution across the five analysed cores. Cores located along the river channel show a bimodal distribution (i.e., silt and clay), with most of the sediments being silt. Core 545, which is located 7.5 km away from the river channel, still has a mostly bimodal distribution, but with most of the sediments being clay. Lake sediments are composed almost exclusively of clay. Measurements were made punctually for each lithological unit.

high between 10,000 and 6000 cal yr BP, with a sharp drop around 6000 cal yr BP and a slight decrease during the late Holocene.

Mineralogical composition as obtained by XRD shows a clear difference between cores 494 and 545 on one side and the lake core 598 on the other (Supplementary Table 2), separated by the fluvial deposits that acted as a dam at the mouth of the valley and formed the lake. The samples in cores 494 and 545 are found to contain two different expansive clay phases with basal spacings around 14 and 12 Å, which can be assigned to smectite and to illite-smectite phases, respectively (oriented aggregate mounts did not allow us to unambiguously identify the interstratified phase, which we tentatively assign to illite-smectite). Lake sediments have very low amounts of illite-smectite and muscovite/illite but presence of $Al(OH)_3$ gibbsite, a mineral that forms due to weathering, which was identified all along the lake core, but is absent in cores 494 and 545. This suggests that sediments mostly come from the catchment of the lake, which comprises extremely weathered soil, and not from fluvial input.

3.4. C, N and their stable isotopes ($\delta^{13}C$ and $\delta^{15}N$)

The average standard deviations of $\delta^{13}C$ and $\delta^{15}N$ in the long run were lower than 0.1 and 0.2 respectively. Organic carbon ranges between 1% and 2% since the formation of the lake until ca. 9200 cal yr BP (Fig. 5), when it increases towards a range between 3% and 4%. A sharp decline follows the 6000 cal yr BP event. Values rise again after 5000 cal yr BP. C/N values, together with $\delta^{13}C$, increase in phase with the peak in sedimentation rate at around 12,200 cal yr BP. Then, they behave in anti-phase after the 10,000 cal yr BP event, with decreasing C/N ratios and increasing $\delta^{13}C$. C/N values keep slightly decreasing from around 7000 cal yr BP until modern times, while $\delta^{13}C$ values stay in the range between −20‰ and −24‰ until around 4000 cal yr BP, then start decreasing slightly (Fig. 6).

4. Discussion

4.1. Lake Formation and evolution. Tectonic vs. climatic signal

Based on the morphology and location of Lake Oceano, we formulated the hypothesis that the lake formed because of a natural dam of fluvial sediments deposited along the right margin of the Mamoré River. The lack of palaeosols, or other types of visible stratigraphic discontinuities along the cores 494 and 545, suggests that the dam formation was a singular, and probably short, event. This is supported by the mineralogy of the 494, 545 and 598 stratigraphic profiles (Figs. 3, 4), which show two different sources of sediments for the dam and for the lake. Had the dam been formed by several depositional events, we would observe pulses of fluvial sediments entering the lake synchronous with these events. On the contrary, the granulometry, mineralogy, colour and

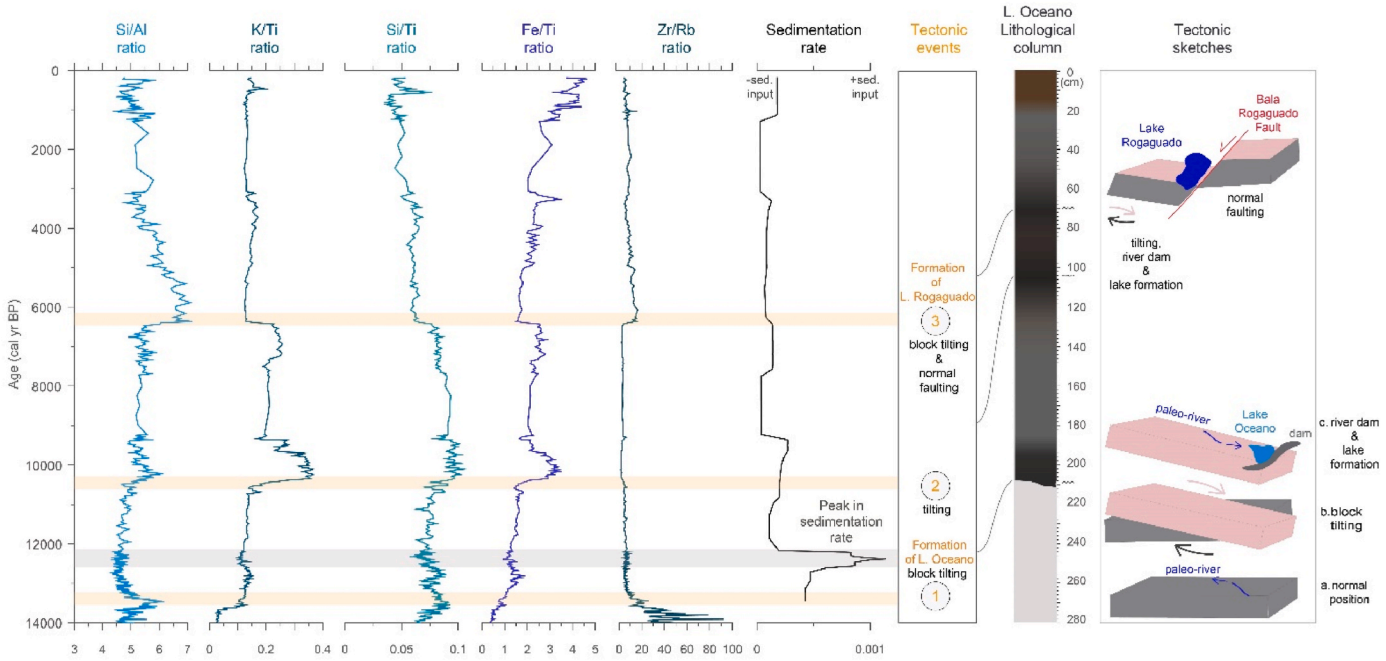

Fig. 4. XRF ratios (blue lines) and sedimentation rate (black line) in logarithmic scale. Major changes in XRF ratios are visible at ~13,435 cal yr BP, marking the formation of the lake, and at ~10,000 and ~6000 cal yr BP. The largest increase in sedimentation rate occurs at around 12,200 cal yr BP; minimum sedimentation rate occurs between 9200 and 7700 cal yr BP. The main tectonic events identified in the sedimentary record are shown in orange. On the right are represented the 598-core lithological column and tectonic sketches showing the tectonic evolution of the area and the lake's formation. (For interpretation of the references to colour in this figure legend, the reader is referred to the Web version of this article.)

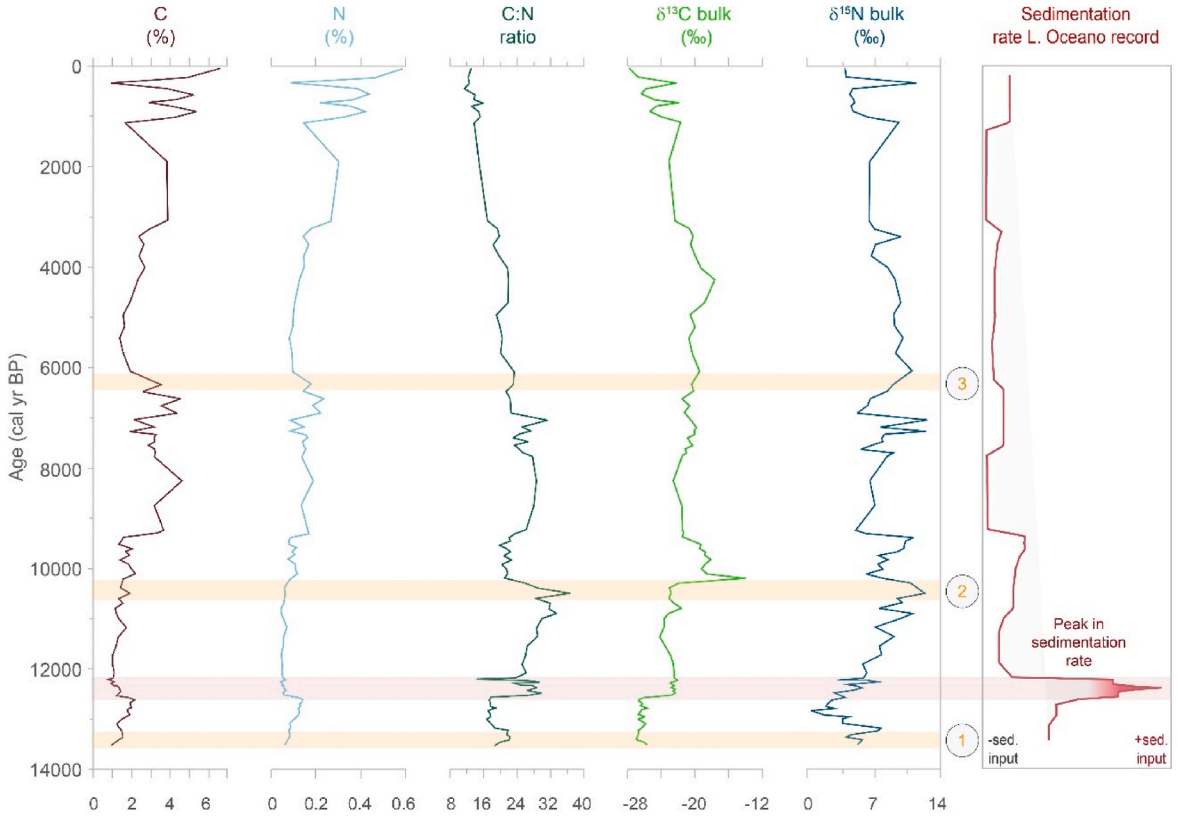

Fig. 5. Lake organic matter. Most of the changes in the amount of C, N, C:N and C and N stable isotopes are consistent with the changes in the XRF ratios shown in Fig. 4. Changes in the organic components and ratios are in phase with the changes in the sedimentation rate (red plot). (For interpretation of the references to colour in this figure legend, the reader is referred to the Web version of this article.)

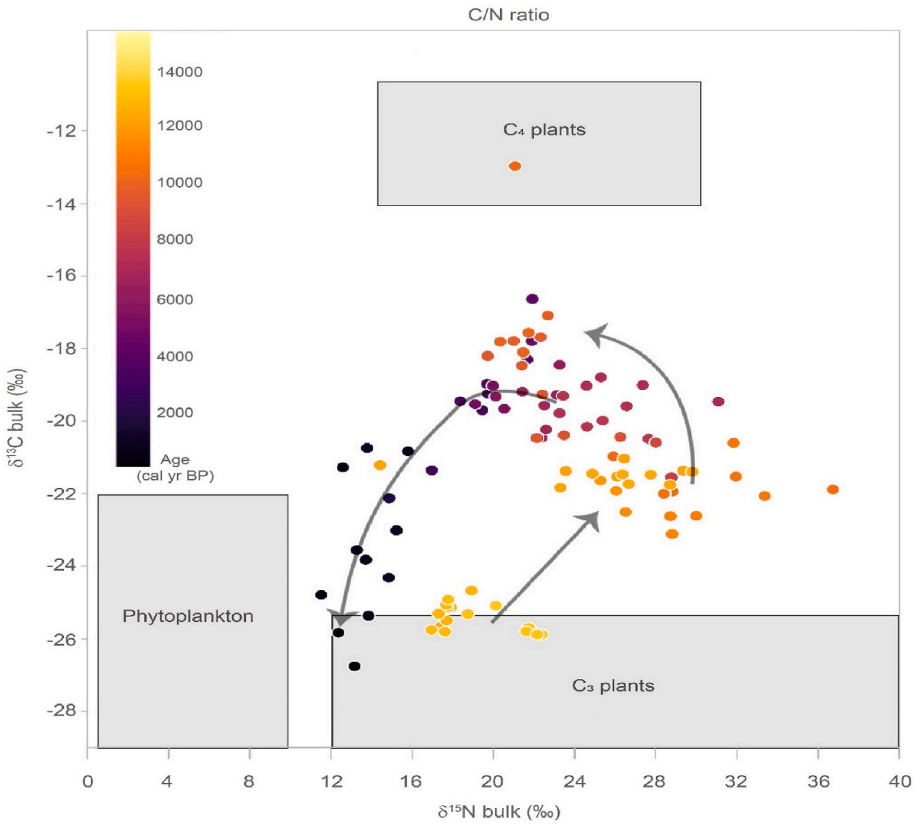

Fig. 6. Scatter plot of ^{13}C versus ^{15}N stable isotopes. Clear shifts in the lake ecology are visible following the 12,200 and 10,000 cal yr BP events. A more continuous change happens after 10,000 cal yr BP.

amount of organic matter in the 598 lake core suggest that the totality of the sediments entering the lake came from the lake catchment, in a low energy environment (i.e., low angle slope, low water energy). Based on the depth of core 494 and the fact that the corer did not reach the floor of the ancient valley, we can establish that the vertical movement that formed Lake Oceano was at least 8 m in magnitude. This is in line with the measured vertical displacements of other faults in the Llanos de Moxos (Lombardo and Grützner, 2021). Our hypothesis for the formation of Lake Oceano is consistent with the granulometry of cores 382 and 310, which is similar to that of core 494, and with the age of the bottom of core 382 (Fig. 3), which approximate the formation of the lake. The three cores are also to the south of the Bala-Rogaguado fault line, and to the east of the Mamoré Fault (Fig. 1), which means they are in the same tectonic sub-block.

River sedimentation patterns are mostly driven by changes in precipitation. Therefore, to identify the main driver of changes in the sedimentation records shown here, we need to compare them with the palaeo-precipitation record. Currently, there are no palaeo-precipitation records reconstructed from the Llanos de Moxos. Precipitation records are, however, available from Lake Titicaca (Baker et al., 2001b), the Salar de Uyuni salt flat (Baker et al., 2001a), the Jaraguá cave (Novello et al., 2017) and Lake La Gaiba (Metcalfe et al., 2014; Whitney, 2011) in the Pantanal region. Overall, these records indicate a dry period between about 15,000 and 13,000 cal yr BP, coinciding with the European Bølling-Allerød interstadial warm period, followed by a short-lived period of high precipitation around 12,000 cal yr BP coinciding with the Younger Dryas stadial. Precipitation decreases again after the Younger Dryas until the beginning of the late Holocene, when a wet phase is established. However, a wet phase between 10,000 and 8500 cal yr BP has been detected in the Lake Titicaca (Baker et al., 2001b). Both the formation of the lake and the burial of the plant remains in core 382 happen during a dry period and, therefore, are most likely explained by the damming of the Mamoré River caused by a downriver uplift on a tilting block belonging to the southern rim of the Fitzcarrald Arch. We can use the age of the beginning of the lacustrine sedimentation of Lake Oceano to date this uplift at around 13,400 cal yr BP. Once the lake formed, subsequent uplift events would change the hydrology of the lake, by raising the water table, or tilting the topography, but did not cause overflow from the river to the lake, nor new overbank sediment deposition at the lake's latitude. Given the negligible slope of the LM of only about 10 cm/km, an uplift of 8 m would have caused far larger landscape transformations than just the formation of Lake Oceano. The reduction in drainage would have caused a far deeper and more prolonged flooding season across a vast swathe of the LM inducing the formation of fluvial distributary systems where rivers reached the flooded areas. Our hypothesis would also explain the presence of several, very thick, early Holocene, clayish palaeosols that outcrop along the Mamoré riverbanks (Lombardo et al., 2018; May et al., 2015). These formed as accretionary soils by seasonal deposition of clay, probably caused by an increase of the river water level coupled with low water velocity (May et al., 2015), which is consistent with our hypothesis of high-water level been caused by northern damming (i.e. uplift due to block tilting) rather than increased precipitation, which would have caused deposition of coarser material. Furthermore, these palaeosols contain abundant red mottling and gypsum crystals (Lombardo et al., 2018). The presence of gypsum crystals indicates evaporation of ground water (Van Breemen and Buurman, 2002). The absence of gypsum in all the modern soils suggests that modern conditions are wetter than the conditions under which these palaeosols formed, further pointing towards a tectonic rather than climatic control on sedimentation patterns.

4.2. Hydrology

To disentangle climatic from tectonic drivers of changes in the lake

deposits, we further looked at the lake and its catchment hydrology. If we disregard tectonics as driver for the lake formation and instead assume an increased precipitation rate, this in turn would lead to increased runoff and sediment supply but with relatively stable mean water level (seasonally averaged), as the lake drains into the Mamoré River any excess water through an outlet stream. This implies that, even during periods of higher precipitation, the distance of the core location from the shoreline would not change significantly. In contrast, a downriver uplift would have raised the water table and the Mamoré River base level, expanding the size of the lake. This would have reduced the size of the lake sedimentary catchment and increased the distance of the core location from the shoreline. Assuming no change in precipitation, this would cause a decrease in sedimentation rate at the core location. We observe a sharp increase in sedimentation rate in Lake Oceano around 12,200 cal yr BP. This event is not associated with any significant change in the elemental ratios or granulometry of the sediments, suggesting that there is no discernible change in the catchment of the lake, nor in the distance of the core location from the shoreline, but only an increased runoff, which we interpret as resulting from an increase in precipitation. This is synchronous with the onset of a period of high variability, with rising water levels, registered also at Laguna La Gaiba, in the Bolivian Pantanal, which is accompanied by an increase of $\delta^{13}C$ values (Metcalfe et al., 2014) and with a wet phase registered in the speleothem as observed at the Jaraguá cave (Novello et al., 2017). Both C/N ratios and $\delta^{13}C$ show a shift towards higher values after 12,200 cal yr BP. The increased runoff can explain the increase in C/N values, as more organic matter would enter the lake from the catchment. The change in $\delta^{13}C$ is more difficult to explain. Palaeo-vegetation reconstructions from south-western Amazonia through the Holocene have consistently associated precipitation increase with ecotonal forest expansion (Mayle et al., 2000), which should cause a shift from C_4-dominated savannah to C_3-dominated forest, with a consequent decrease of $\delta^{13}C$. The increase in atmospheric CO_2 values observed at the transition from the LGM to the Holocene should also favour C_3 plants and contribute towards lower $\delta^{13}C$ values as observed by Novello et al. at the Jaraguá cave (Novello et al., 2019). A possible explanation could be that $\delta^{13}C$ values are due to increased eutrophic levels resulting from increased nutrient supply (Brenner et al., 1999) during a period of higher runoff. Another possible driver of increased sediment supply could have been megafauna overgrazing. In contrast with the flat landscape of the LM, the surroundings of Lake Oceano are characterised by gentle slopes, therefore offering high ground refugia for the megafauna during the period of increased precipitation and flooding during the Younger Dryas. Megafauna overgrazing would have reduced the vegetation cover and increased the erosion of the catchment in coincidence of increased precipitation. The third important change in sediment parameters happened around 10,200 cal yr BP, accompanied by an increase in Si/Al, K/Ti, K/Al, and Si/Ti ratios, a sharp decrease in C/N, and a further increase in $\delta^{13}C$. All these changes lasted for about 1000 years and reverted to pre-10,200 cal yr BP conditions around 9200 cal yr BP. The increase in C/N values suggests a shift in the source of sediment organic matter, with increasing contribution from algae relative to terrestrial plants from the catchment (Brenner et al., 1999; Giesche et al., 2021). This shift could be due to an increase in the water level, which would increase the distance between the core location and the shoreline. This scenario is consistent with the increase in Fe/Ti, which indicates more reducing conditions, and a decrease in Zr/Rb, which indicates inputs of lighter material; as suspended sediments must travel a longer distance to reach the core location, heavier material is less likely to travel to the core location. The change in $\delta^{13}C$ can also be caused by changes in the water level, as these would have had a big impact over the lake ecology.

4.3. Aquatic vegetation feedback to changes in hydrology

Shallow tropical lakes like Lake Oceano shift towards clear waters and abundance of free-floating aquatic plants and submerged macrophytes during periods of high-water levels and toward increasing turbidity and blooms of nitrogen-fixing cyanobacteria during periods of lower-water levels (Loverde-Oliveira, 2009; O'Farrell, 2011). Bolivian lakes reach minimum water levels at the peak of the dry season, when strong winds from the south generate waves that can remobilize shoreline sediments (Lombardo and Veit, 2014). During periods when mean water level is higher, the frequency and intensity of shoreline sediment mobilisation is reduced, allowing for the establishment of clear-water conditions and expansion of submerged macrophytes, which, through positive feedback, contribute to the maintenance of clear-water conditions all year around (Loverde-Oliveira, 2009; Su, 2019). High water level following the uplift is maintained until the Mamoré River incises the bedrock, increasing the drainage of the LM and lowering the water table back to its pre-uplift depth. Based on the signal from elemental ratios around 10,000 cal yr BP, we can infer that the Mamoré incision lasted around 1000 years. Our interpretation does not exclude the possibility of a climate contribution to these lake-level changes. In fact, an increase in precipitation between 10,000 and 8500 cal yr BP caused overflow from Lake Titicaca (Baker et al., 2001b). It could also explain the increase in sedimentation rate at Lake Oceano between 10,000 and 9300 cal yr BP. However, the drop in the sedimentation rate after 9200 cal yr BP, which coincides with a sharp change in almost all the other proxies (due to evaporation and weathering), suggests a dry period, rather than a wet one for this time interval (Fig. 4). A dry period beginning at ca. 10,000 cal yr BP is also recorded at Laguna La Gaiba by an expansion of dry forest taxa and shallow-water *Pediastrum* algae between 10,000 and 3000 cal yr BP (Whitney, 2011; Whitney and Mayle, 2012). The latest event, clearly marked by sharp shifts in the elemental ratios, coincides with the formation of Lake Rogaguado at around 6000 cal yr BP (Giesche et al., 2021; Lombardo, 2014).

4.4. Regional events

Lake Rogaguado, located 130 km south-west of Lake Oceano, formed inside a palaeo-valley of the Beni River due to slope inversion, after an uplift of at least 2 m towards the north (Lombardo, 2014). The 13,400 and 10,000 cal yr BP uplift events registered in Lake Oceano core are both characterised by increases in Si/Al, K/Ti, Si/Ti, and Fe/Ti and decrease in Zr/Rb elemental ratios. Except for the Si/Al ratio, all the other elemental ratios also show shifts at 6000 cal yr BP, but in the opposite direction to those at 13,400 and 10,000 cal yr BP. The increase in the Si/Al ratio is consistent with a shift towards coarser material, similar to the Lake Rogaguado core. The exact location of the fault that caused the formation of Lake Rogaguado is unknown, but it could be a transfer fault associated with the Bala-Rogaguado fault line (which is the master fault). This fault might be located north of Lake Oceano (red dashed line in Fig. 1b), passing north of the Puerto Siles knickpoint (Fig. 5 in Lombardo, 2014) and would have caused Lake Oceano to be uplifted as well, with consequences over its catchment topography and reduction in its water level.

A peak in aridity around 6000 cal yr BP, which is present in most records across SW Amazonia (Smith and Mayle, 2017; Wang, 2017), could have also triggered a decrease in sedimentation rates caused by lower precipitation and an increase in grain size caused by a shorter distance between the shoreline and the core location. However, the fact that the changes observed around 6000 cal yr BP are abrupt, and coincide with the formation of Lake Rogaguado, suggests that they have been mainly triggered by a neotectonic event, rather than climate change. We plan to analyse pollen and other palynomorphs in the future, to help understand the type and causes of vegetation change in the region. However, to better constrain the effects of neotectonics on landscape evolution of the LM more mapping and coring are needed. Future research should focus on: i) dating the formation of the fluvial distributary systems formed inside the LM and establishing the extent to which their formation has been induced by upriver uplifts, and ii)

reconstructing a palaeo-precipitation curve from the LM covering the last 15,000 years.

5 Conclusions

We show that ria lakes can provide key sedimentary archives for reconstructing the timing and intensity of both Late Quaternary tectonic and climate events. The savannah landscape of the Bolivian Llanos de Moxos in SW Amazonia is highly dynamic. Its evolution is controlled by the interplay between Holocene (interglacial) climatic change and neotectonic events. Here, we have identified a new uplift event at around 13,400 cal yr BP, with an 8 m minimum vertical displacement, which formed Lake Oceano. At this lake we also find evidence for a second uplift event at around 10,000 cal yr BP, coinciding with a marked shift in lake sediment geochemistry, and a third uplift event at 6000 cal yr BP, which formed Lake Rogaguado—one of the largest lakes in South America. At Lake Oceano we also found a sharp increase in the sedimentation rate at 12,200 cal yr BP, which is consistent with a period of high precipitation during the Younger Dryas. We show that these events had a noticeable impact on the trophic status of the lake, as inferred from the changes in $\delta^{13}C$, $\delta^{15}N$ and C:N ratios. Our study shows the importance of considering, not only climate change, but also neotectonics, when seeking to understand the flood history of this archaeologically and biologically important region.

Author contribution

All authors made substantial contributions to the manuscript. U.L. designed the research. U.L. and H.V. conducted the fieldwork and interpreted the stratigraphic profiles. L.B-V and C.B. R. dated the cores, did the age-depth model and sedimentation rate, U.L. and G.B. analysed the XRF data and produced figures. J. I-I analysed the clay mineralogy. UL performed and interpreted the granulometric, stable isotopes and C:N analyses. U.L., F. M. and H.V. secured the funding. U.L. and F.M. wrote the first version of the manuscript with the help of all the coauthors. U.L. and G.B. produced the revised and final version of the manuscript. All authors have approved the final version of the manuscript.

Declaration of Competing Interest

The authors declare that they have no known competing financial interests or personal relationships that could have appeared to influence the work reported in this paper.

Acknowledgements

This work was supported by Swiss National Science Foundation grant numbers 200020–141277/1 and P300P2_158459/1; Marie Skłodowska-Curie Actions EU Project 703045A; AHRC-FAPESP MoU research grant HERCA, reference AH/S001662/1; the ERC Consolidator project DEMODRIVERS funded by the European Research Council (ERC), project Nº 101043738. This article contributes to ICTA-UAB 'María de Maeztu Unit of Excellence' (CEX2019-000940-M). This work also contributes to EarlyFoods (Evolution and impact of early food production systems), which has received funding from the Agència de Gestió d'Ajuts Universitaris i de Recerca de Catalunya (SGR-Cat-2021, 00527). This research was supported by grant PID2022-138350OA-I00, funded by MICIU/AEI/10.13039/501100011033/ and ERDF "A way of making Europe", EU. We thank Soledad Alvarez Pousa from GEO3BCN-CSIC for assistance with the XRD measurements, Elena Martinez Planchart from CSIC - ICM Geologia Marina in Barcelona for helping with the grain size analysis, Hendrik Vogel for assistance with the XRF measurements at the University of Bern; and Ezequiel Chavez for assisting with lake coring and export of samples. We thank the Bolivian Ministry of the Environment and Water, and the Noel Kempff Mercado Natural History Museum, for permission (no. 0342/2019) to collect the sediment cores and export them to Europe for analysis.

Appendix A. Supplementary data

Supplementary data to this article can be found online at https://doi.org/10.1016/j.quascirev.2025.109197.

Data availability

All data and/or code is contained within the submission.

References

Baker, P.A., Rigsby, C.A., Seltzer, G.O., Fritz, S.C., Lowenstein, T.K., Bacher, N.P., Veliz, C., 2001a. Tropical climate changes at millennial and orbital timescales on the Bolivian Altiplano. Nature 409 (6821), 698–701.

Baker, P.A., Seltzer, G.O., Fritz, S.C., Dunbar, R.B., Grove, M.J., Tapia, P.M., Cross, S.L., Rowe, H.D., Broda, J.P., 2001b. The history of South American tropical precipitation for the past 25,000 years. Science 291, 640–643.

Boixadera, J., Poch, R.M., García-González, M.T., Vizcayno, C., 2003. Hydromorphic and clay-related processes in soils from the Llanos de Moxos (northern Bolivia). Catena 54, 403–424.

Brenner, M., Whitmore, T.J., Curtis, J.H., Hodell, D.A., Schelske, C.L., 1999. Stable isotope (δ13C and δ15N) signatures of sedimented organic matter as indicators of historic lake trophic state. J. Paleolimnol. 22, 205–221.

Bronk Ramsey, C., 2009. Dealing with outliers and offsets in radiocarbon dating. Radiocarbon 51, 1023–1045.

Davies, S.J., Lamb, H.F., Roberts, S.J., 2015. Micro-XRF core scanning in palaeolimnology: recent developments. In: Croudace, I.W., Rothwell, R.G. (Eds.), Micro-XRF Studies of Sediment Cores. Springer, Netherlands, pp. 189–226.

Dumont, J.F., 1993a. Lake patterns as related to neotectonics in subsiding basins: the example of the Ucamara Depression, Peru. Tectonophysics 222, 69–78.

Dumont, J.F., 1993b. Type of lakes as related to neotectonics in western Amazonia. International Symposium on the Quaternary of Amazonia, 8-13 November 1992. Universidade de Amazonas, Manaus, Brazil.

Dumont, J.F., 1996. Neotectonics of the Subandes-Brazilian craton boundary using geomorphological data: the Marañon and Beni basins. Tectonophysics 257, 137–151.

Dumont, J.F., Fournier, M., 1994. Geodynamic environment of Quaternary morphostructures of the subandean foreland basins of Peru and Bolivia: characteristics and study methods. Quat. Int. 21, 129–142.

Dumont, J.F., Guyot, J.L., 1993. Ria lac: ou, pourquoi? Proceedings of the Third International Conference on Geomorphology, 23-29 August, 1993, Hamilton, Canada.

Espurt, N., Baby, P., Brusset, S., Roddaz, M., Hermoza, W., Barbarand, J., 2010. The Nazca Ridge and uplift of the Fitzcarrald Arch: implications for regional geology in northern South America. In: Hoorn, C., Wesselingh, F.P. (Eds.), Amazonia: Landscape and Species Evolution. Wiley-Blackwell Publishing Ltd., Oxford, UK, pp. 89–100.

Espurt, N., Baby, P., Brusset, S., Roddaz, M., Hermoza, W., Regard, V., Antoine, P.O., Salas-Gismondi, R., Bolaños, R., 2007. How does the Nazca Ridge subduction influence the modern Amazonian foreland basin? Geology 35, 515–518.

Giesche, A., Lombardo, U., Finsinger, W., Veit, H., 2021. Reconstructing Holocene landscape and environmental changes at lago Rogaguado, Bolivian Amazon. J. Paleolimnol. 65, 235–253.

Guyot, J.L., Jouanneau, J.M., Wasson, J.G., 1999. Characterisation of river bed and suspended sediments in the Rio Madeira drainage basin (Bolivian Amazonia). J. S. Am. Earth Sci. 12, 401–410.

Hanagarth, W., 1993. Acerca de la geoecología de las sabanas del Beni en el noreste de Bolivia. Instituto de ecología, La Paz.

Hogg, A.G., Heaton, T.J., Hua, Q., Palmer, J.G., Turney, C.S.M., Southon, J., Bayliss, A., Blackwell, P.G., Boswijk, G., Bronk Ramsey, C., Pearson, C., Petchey, F., Reimer, P., Reimer, R., Wacker, L., 2020. SHCal20 southern hemisphere calibration, 0–55,000 Years cal BP. Radiocarbon 62, 759–778.

Horton, B.K., Capaldi, T.N., Perez, N.D., 2022. The role of flat slab subduction, ridge subduction, and tectonic inheritance in Andean deformation. Geology 50, 1007–1012.

Junk, W., 2013. Current state of knowledge regarding South American wetlands and their future under global climate change. Aquatic Sciences - Research Across Boundaries 75, 113–131.

Junk, W.J., Bayley, P.B., Sparks, R.E., 1989. The Flood Pulse Concept in River-Floodplain Systems, vol. 106. Canadian special publication of fisheries and aquatic sciences, pp. 110–127.

Langstroth, R.P., 2011. Biogeography of the Llanos de Moxos: natural and anthropogenic determinants. Geograph. Helv. 66, 183–192.

Lombardo, U., 2014. Neotectonics, flooding patterns and landscape evolution in southern Amazonia. Earth Surf. Dyn. 2, 493–511.

Lombardo, U., 2016. Alluvial plain dynamics in the southern Amazonian foreland basin. Earth System Dynamics 7, 453–467.

Lombardo, U., Canal-Beeby, E., Veit, H., 2011. Eco-archaeological regions in the Bolivian Amazon: linking pre-Columbian earthworks and environmental diversity. Geograph. Helv. 66, 173–182.

Lombardo, U., Denier, S., May, J.-H., Rodrigues, L., Veit, H., 2013a. Human–environment interactions in pre-Columbian Amazonia: The case of the Llanos de Moxos, Bolivia. Quat. Int. 312, 109–119.
Lombardo, U., Denier, S., Veit, H., 2015. Soil properties and pre-Columbian settlement patterns in the Monumental Mounds Region of the Llanos de Moxos, Bolivian Amazon. SOIL 1, 65–81.
Lombardo, U., Grützner, C., 2021. Tectonic geomorphology and active faults in the Bolivian Amazon. Global Planet. Change 203, 103544.
Lombardo, U., Iriarte, J., Hilbert, L., Ruiz-Pérez, J., Capriles, J.M., Veit, H., 2020. Early Holocene crop cultivation and landscape modification in Amazonia. Nature 581, 190–193.
Lombardo, U., Rodrigues, L., Veit, H., 2018. Alluvial plain dynamics and human occupation in SW Amazonia during the Holocene: a paleosol-based reconstruction. Quat. Sci. Rev. 180, 30–41.
Lombardo, U., Szabo, K., Capriles, J.M., May, J.-H., Amelung, W., Hutterer, R., Lehndorff, E., Plotzki, A., Veit, H., 2013b. Early and middle Holocene hunter-gatherer occupations in western Amazonia: the hidden shell middens. PLoS One 8, e72746.
Lombardo, U., Veit, H., 2014. The origin of oriented lakes: evidence from the Bolivian Amazon. Geomorphology 204 (0), 502–509.
Loverde-Oliveira, S.M., et al., 2009. Hydrology-driven regime shifts in a shallow tropical lake. Ecosystems 12 (5), 807–819.
May, J.-H., Plotzki, A., Rodrigues, L., Preusser, F., Veit, H., 2015. Holocene floodplain soils along the Río Mamoré, northern Bolivia, and their implications for understanding inundation and depositional patterns in seasonal wetland settings. Sediment. Geol. 330, 74–89.
Mayle, F.E., Burbridge, R., Killeen, T.J., 2000. Millennial-scale dynamics of southern Amazonian rain forests. Science 290, 2291–2294.
Mayle, F.E., Langstroth, R.P., Fisher, R.A., Meir, P., 2007. Long-term forest-savannah dynamics in the Bolivian Amazon: implications for conservation. Phil. Trans. Biol. Sci. 362, 291–307.
Metcalfe, S.E., Whitney, B.S., Fitzpatrick, K.A., Mayle, F.E., Loader, N.J., Street-Perrott, F.A., Mann, D.G., 2014. Hydrology and climatology at Laguna La Gaiba, lowland Bolivia: complex responses to climatic forcings over the last 25 000 years. J. Quat. Sci. 29, 289–300.
Navarro, G., 2011. Clasificación de la vegetación de Bolivia. Centro de ecología difusión fundación Simón I. Patiño, Santa Cruz, Bolivia.
Nichols, G., Fisher, J., 2007. Processes, facies and architecture of fluvial distributary system deposits. Sediment. Geol. 195, 75–90.
Novello, V.F., Cruz, F.W., McGlue, M.M., Wong, C.I., Ward, B.M., Vuille, M., Santos, R.A., Jaqueto, P., Pessenda, L.C.R., Atorre, T., Ribeiro, L.M.A.L., Karmann, I., Barreto, E.S., Cheng, H., Edwards, R.L., Paula, M.S., Scholz, D., 2019. Vegetation and environmental changes in tropical South America from the last glacial to the Holocene documented by multiple cave sediment proxies. Earth Planet Sci. Lett. 524, 115717.
Novello, V.F., Cruz, F.W., Vuille, M., Stríkis, N.M., Edwards, R.L., Cheng, H., Emerick, S., de Paula, M.S., Li, X., Barreto, E.d.S., Karmann, I., Santos, R.V., 2017. A high-resolution history of the southSouth American monsoon from last glacial maximum to the Holocene. Sci. Rep. 7, 44267.
O'Farrell, I., et al., 2011. Water level as the main driver of the alternation between a free-floating plant and a phytoplankton dominated state: a long-term study in a floodplain lake. Aquatic Sci. 73 (2), 275–287.
Pansu, M., Gautheyrou, J., 2006. Handbook of Soil Analysis. Springer-Verlag, Heidelberg.
Regard, V., Lagnous, R., Espurt, N., Darrozes, J., Baby, P., Roddaz, M., Calderon, Y., Hermoza, W., 2009. Geomorphic evidence for recent uplift of the Fitzcarrald Arch (Peru): a response to the Nazca Ridge subduction. Geomorphology 107, 107–117.
Reimer, P.J., Austin, W.E.N., Bard, E., Bayliss, A., Blackwell, P.G., Bronk Ramsey, C., Butzin, M., Cheng, H., Edwards, R.L., Friedrich, M., Grootes, P.M., Guilderson, T.P., Hajdas, I., Heaton, T.J., Hogg, A.G., Hughen, K.A., Kromer, B., Manning, S.W., Muscheler, R., Palmer, J.G., Pearson, C., van der Plicht, J., Reimer, R.W., Richards, D.A., Scott, E.M., Southon, J.R., Turney, C.S.M., Wacker, L., Adolphi, F., Büntgen, U., Capano, M., Fahrni, S.M., Fogtmann-Schulz, A., Friedrich, R., Köhler, P., Kudsk, S., Miyake, F., Olsen, J., Reinig, F., Sakamoto, M., Sookdeo, A., Talamo, S., 2020. The IntCal20 northern hemisphere radiocarbon age calibration curve (0–55 cal kBP). Radiocarbon 62, 725–757.
Rocha, I.S., Machado, R., Santos Júnior, C.R.d., Oliveira, J.R.S.d., Pessi, D.D., Salamuni, E., Ruiz, A.S., Filho, Paranhos, Conceição, A., 2022. Bacia do pantanal revisitada: uma estrutura do tipo rifte relacionada com a migração para sul da subducção sub-horizontal dos andes entre o paleógeno e neógeno. Bol. Parana. Geocienc. 80, 227–241.
Roddaz, M., Baby, P., Brusset, S., Hermoza, W., Maria Darrozes, J., 2005. Forebulge dynamics and environmental control in Western Amazonia: the case study of the Arch of Iquitos (Peru). Tectonophysics 399, 87–108.
Rodrigues, L., Lombardo, U., Canal Beeby, E., Veit, H., 2017. Linking soil properties and pre-Columbian agricultural strategies in the Bolivian lowlands: the case of raised fields in Exaltación. Quat. Int. 437 (Part B), 143–155.
Ronchail, J., Bourrel, L., Cochonneau, G., Vauchel, P., Phillips, L., Castro, A., Guyot, J., Deoliveira, E., 2005. Inundations in the Mamoré basin (south-western Amazon—Bolivia) and sea-surface temperature in the pacific and atlantic oceans. J. Hydrol. 302, 223–238.
Schumm, S.A., Dumont, J.F., Holbrook, J.M., 2002. Active Tectonics and Alluvial Rivers. Cambridge University Press.
Smith, R.J., Mayle, F.E., 2017. Impact of mid- to late Holocene precipitation changes on vegetation across lowland tropical South America: a paleo-data synthesis. Quat. Res. 89 (1), 134–155.
Su, H., et al., 2019. Morphological traits of submerged macrophytes reveal specific positive feedbacks to water clarity in freshwater ecosystems. Science of the Total Environment 684, 578–586.
Van Breemen, N., Buurman, P., 2002. Soil Formation, second ed. Springer.Science+ Businness Media, B.V.
Wang, X., et al., 2017. Hydroclimate changes across the Amazon lowlands over the past 45,000 years. Nature 541 (7636), 204–207.
Whitney, B.S., et al., 2011. A 45 kyr palaeoclimate record from the lowland interior of tropical South America. Palaeogeogr. Palaeoclimatol. Palaeoecol. 307 (1–4), 177–192.
Whitney, B.S., Mayle, F.E., 2012. Pediastrum species as potential indicators of lake-level change in tropical South America. J. Paleolimnol. 47 (4), 601–615.